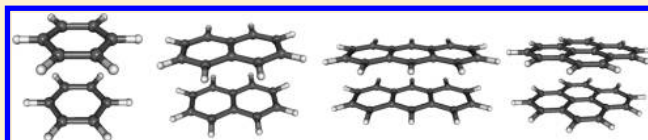


Aromatic Excimers: *Ab Initio* and TD-DFT StudyMaciej Kołaski,[†] C. R. Arunkumar, and Kwang S. Kim*

Center for Superfunctional Materials, Department of Chemistry, Pohang University of Science and Technology, San 31, Hyojadong, Namgu, 790-784 Pohang, Korea

S Supporting Information

ABSTRACT: Excited dimers (excimers) formed by aromatic molecules are important in biological systems as well as in chemical sensing. The structure of many biological systems is governed by excimer formation. Since theoretical studies of such systems provide important information about mutual arrangement of aromatic molecules in structural biology, we carried out extensive calculations on the benzene excimer using EOM-CCSD, RI-CC2, CASPT2, and TD-DFT approaches. For the benzene excimer, we evaluate the reliability of the TD-DFT method based on the B3LYP, PBE, PBE0, and ω PBEh functionals. We extended the calculations to naphthalene, anthracene, and pyrene excimers. We find that nearly parallel stacked forms are the minimum energy structure. On the basis of the benzene to pyrene excimers, we might roughly estimate the equilibrium layer-to-layer distance for bilayer-long arenes in the first singlet excited state, which is predicted to be bound.



■ INTRODUCTION

Excimers, dimers associated with excited electronic states, appear as broad and structureless fluorescence bands in the emission spectra. In the majority of cases, the ground electronic states of excimers are dissociative. Aromatic molecules form excimers in fluid solutions, liquids, molecular crystals, and polymers. Excimer formation is determined by the configurational mixing of exciton and charge resonance states. There are two types of molecular interactions which can contribute to excimer formation: exciton resonance (ER) caused by strong dipole–dipole/multipole–multipole interaction between excited and ground electronic states ($A^*B \leftrightarrow AB^*$) and charge resonance (CR) due to electrostatic interaction between positively and negatively charged ionic states ($A^+B^- \leftrightarrow A^-B^+$). The excimer states originate from complementary contributions of ER and CR states.¹ On the basis of generalized valence bond theory (GVB), the exciton resonance is related to covalent components of the wave function. The charge resonance corresponds to ionic contributions. Theoretical considerations suggest that the binding in molecular excimers is essentially due to the exciton resonance with smaller contributions coming from charge resonance. However, in the case of many molecular excimers, the source of stabilization is widely debated. This simplified model of excimer formation which is based on the ER and CR resonances in many cases cannot properly explain some experimental results, and mixing of two configurations provides much better description. In the latter case, the localized orbitals of the excimer are expressed as normalized linear combinations of ER and CR resonances ($2^{-1/2}(A^*B - AB^*)$, $2^{-1/2}(A^*B + AB^*)$, $2^{-1/2}(A^+B^- - A^-B^+)$, and $2^{-1/2}(A^+B^- + A^-B^+)$).

Excimers are usually dimeric species formed between two identical atoms or molecules which are weakly bound in their ground electronic states. The lifetime of an excimer is short, on the order of nanoseconds. Heterodimeric diatomic dimers

involving noble gas and halide such as xenon chloride, which are often used for excimer lasers, are widely employed in microsurgery. These lasers take advantage of the fact that exciplex (excited complex) components have attractive interactions in the excited state, while the ground state interactions are repulsive. The excimer formation has been an important topic in molecular sensing.^{2,3} The formation of pyrene has many applications in biophysics and structural biology.^{4–7} It allows for determining the distance between biomolecules.⁸ Besides the technological use of their fluorescence, excimers formed by aromatic hydrocarbons are involved in important photochemical reactions like photo-dimerization and photolysis.

Aromatic hydrocarbons are planar, and their most stable excimer structure is usually perfectly stacked, which is related to a symmetric pair of parallel molecules. The pyrene dimer was the first experimentally studied aromatic system which forms a stable excimer.⁹

Moreover, excimer formation was shown to be a photo-physical phenomenon characteristic for various aromatic molecules.¹⁰ The potential energy curves showing the ground state and the lowest excited singlet electronic states of the aromatic molecules as a function of intermonomer distance between monomers are usually employed to explain the phenomenon of excimer formation (see Figure 1).¹¹

Two lowest singlet excited states of the benzene dimer are described by B_{1g} and B_{2u} states. The dominant transition for the B_{1g} state involves the HOMO→LUMO ($e_{1g} \rightarrow e_{2g}$) excitation. The two highest occupied orbitals for the benzene dimer are doubly degenerate: e_{1g} and e_{1u} orbitals. The e_{1g} is denoted as the HOMO and the e_{1u} is designated as the HOMO–1. The two lowest unoccupied benzene dimer orbitals are also doubly

Received: May 3, 2012

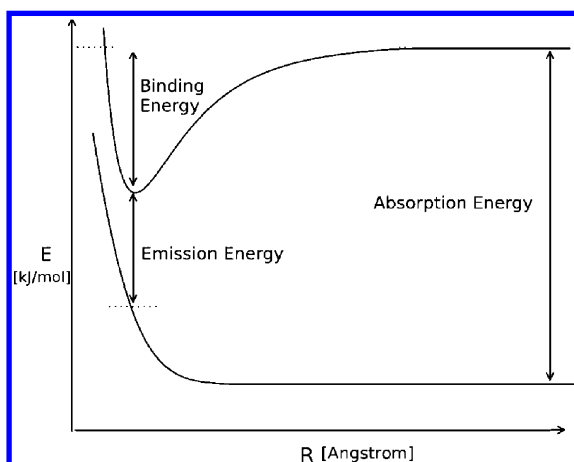


Figure 1. Schematic diagram of the potential energy curves of the ground and the first excited state (excimer state). The meaning of the binding, emission, and absorption energies is explained.

degenerate e_{2g} (LUMO) and e_{2u} (LUMO+1) orbitals. The dominant transition for the B_{2u} state is also the HOMO→LUMO ($e_{1g} \rightarrow e_{2g}$) transition.^{12–15} The benzene excimer is formed in the B_{1g} state; the B_{2u} state is repulsive. The

HOMO→LUMO excitation makes the interaction between benzene rings stronger due to the increased orbital overlap between monomers. The lowest singlet excited state B_{3g} for the naphthalene dimer is determined by the HOMO→LUMO ($a_u \rightarrow b_{2g}$) transition. The B_{2g} , B_{2u} , and B_{3u} singlet excited states are characterized by various combinations of HOMO→LUMO+1 ($a_u \rightarrow b_{3g}$) and HOMO–1→LUMO ($b_{1u} \rightarrow b_{2g}$) as well as HOMO–1→LUMO+1 ($b_{1u} \rightarrow b_{3g}$) transitions. The lowest singlet excited state B_{3g} for the anthracene dimer is determined by the HOMO→LUMO ($b_{1g} \rightarrow b_{3u}$) excitation. The B_{2g} , B_{2u} , and B_{3u} singlet excited states are characterized by combinations of HOMO→LUMO+1 ($b_{1g} \rightarrow a_u$) and HOMO–1→LUMO ($b_{2g} \rightarrow b_{3u}$) as well as HOMO–1→LUMO+1 ($b_{2g} \rightarrow a_u$) transitions. In the case of the pyrene dimer, the lowest B_{2g} singlet excited state is determined by the HOMO→LUMO ($b_{3g} \rightarrow a_u$) transition. The B_{2g} , B_{2u} , and B_{3u} excited states are combinations of HOMO→LUMO+1 ($b_{3g} \rightarrow b_{1u}$), HOMO–1→LUMO ($b_{2g} \rightarrow a_u$), and HOMO–1→LUMO+1 ($b_{2g} \rightarrow b_{1u}$) transitions. The frontier orbitals of benzene, naphthalene, and pyrene monomers are presented in Figure 2. Although excimers formed by aromatic molecules are important in many different fields, their interaction energies, geometrical parameters, and molecular properties are still scarce. In particular, the excimer

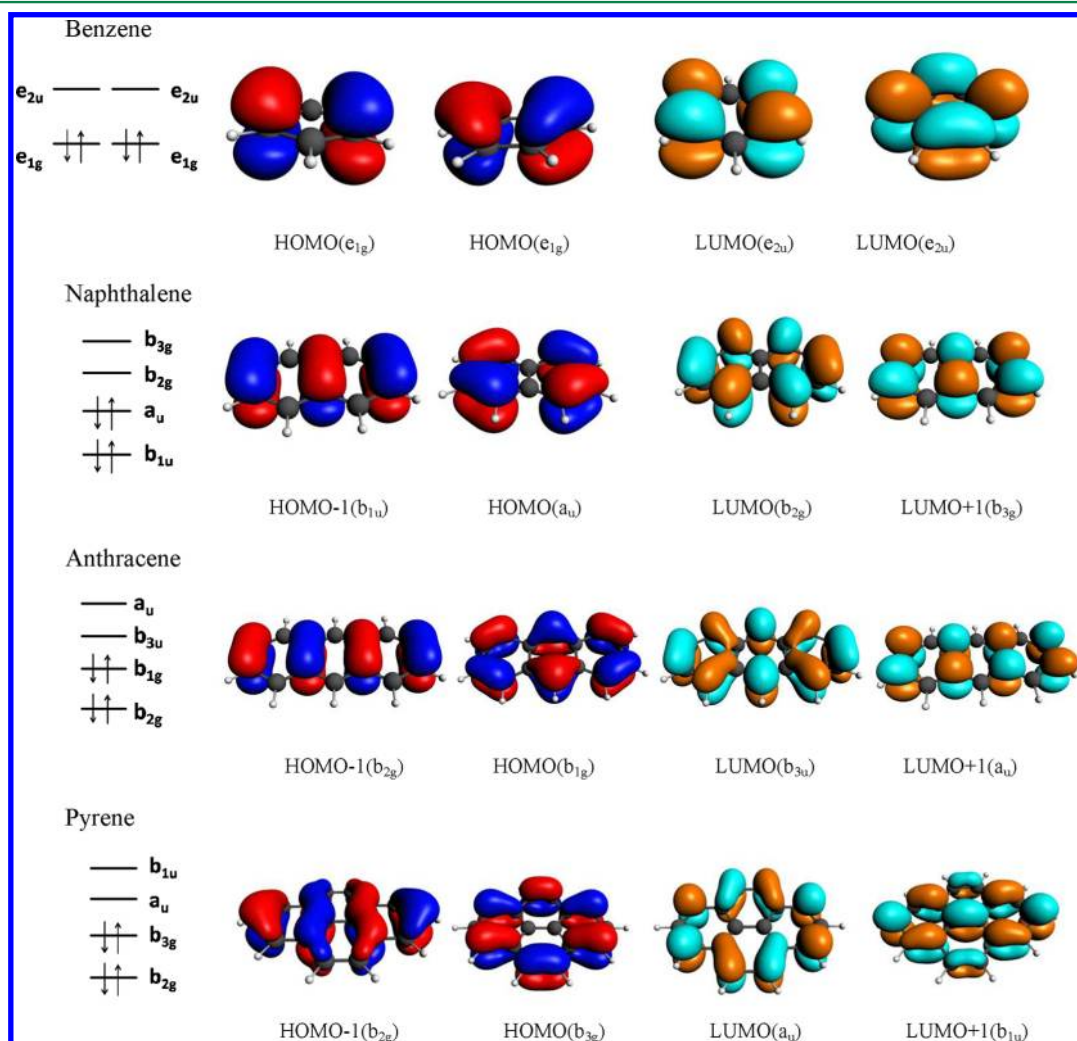


Figure 2. Frontier molecular orbitals (FMOs) for the benzene, naphthalene, and pyrene monomers. For each molecular orbital, we assign appropriate irreducible representation. The schematic arrangement of FMOs is also described.

formation of a graphene bilayer and the structure and properties would also be an interesting study, as graphene is a highly useful material.^{16–26}

Aromatic excimers are difficult to study theoretically. Most theoretical studies in the early stage of this research employed semiempirical methods.^{27–29} While the distance between monomers is large, the static correlation plays an important role, and multiconfigurational methods work much better. The CASPT2 approach is a very useful tool for studying such molecular systems; however, this is a very expensive computational method. It can be used only for limited active space size. The RI-CC2 approach is much faster in comparison with the CASPT2 method; however, for quasi-degenerate systems, the RI-CC2 method usually encounters convergence problems.

COMPUTATIONAL DETAILS

We carried out calculations of benzene, naphthalene, anthracene, and pyrene excimers (Figure 3). Throughout the

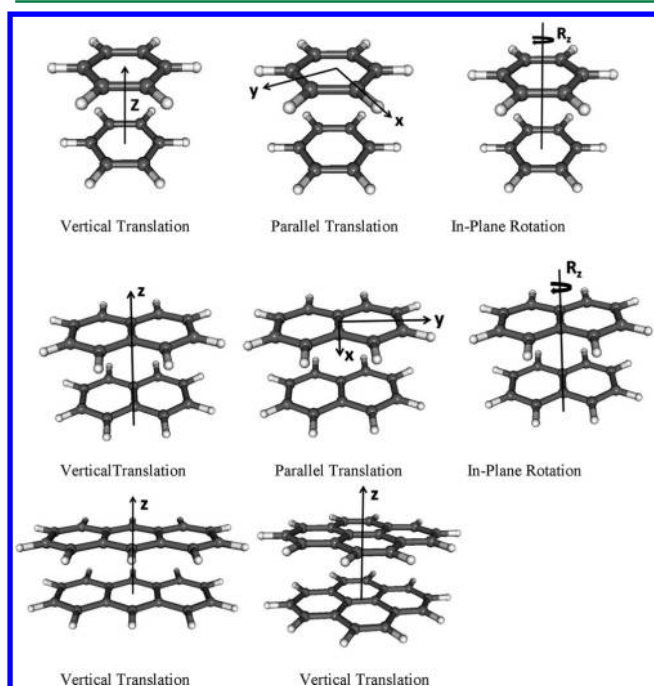


Figure 3. Cartesian coordinate system along with the three basic types of geometrical distortions examined for the benzene, naphthalene, anthracene, and pyrene excimers. The translational coordinates are labeled x , y , and z , and the clockwise rotational coordinate is denoted as R_z .

present work, all the atoms were treated with the aug-cc-pVDZ basis set (which we have abbreviated as aVDZ). For the benzene excimer, we carried out calculations using many different computational approaches. It enables us to obtain its accurate equilibrium intermolecular distances, binding energy, and emission energy. We calculated the potential energy curves for B_{1g} and B_{2u} states of the benzene dimer using CASPT2,^{10,30} RI-CC2,^{11,31} EOM-CCSD,^{32,33} and TD-DFT (Time Dependent Density Functional Theory) methods. CASPT2 computations are based on the CASSCF method with the CAS(12e,12o) active space. The active space includes all π and π^* molecular orbitals. Recently, Inagaki et al.³⁴ performed multiconfiguration quasi-degenerate perturbation theory (MCQDPT)³⁵ calculations based on the CASSCF expansion for an identical group of

aromatic excimers. They considered HOMO–1, HOMO, LUMO, and LUMO+1 molecular orbitals, since their active space was CAS(8e,8o). By using a very limited size of the active space, such computations are feasible to perform even for the pyrene excimer. However, the overall accuracy is slightly sacrificed in the case of large excimers. Benzene and pyrene excimers were studied by using the TD-DFT method based on the BH-LYP hybrid functional with the TZVP basis set,¹⁴ which are in qualitative agreement with the experimental data. In the case of the TD-DFT approach, we employed B3LYP,³⁶ PBE,³⁷ and PBE0³⁸ functionals.

The comparison of TD-DFT results with more accurate approaches would verify the reliability of various DFT functionals for aromatic excimers. TD-DFT is much faster compared to more accurate approaches, applicable for significantly larger systems. It is important to prove that the parallel stacked conformer forms the most stable structure. The most stable conformation of the benzene excimer is determined by the minimum on the potential energy curve for the B_{1g} state. Thus, for the most stable benzene excimer, we calculated the potential energy curves for slipped-parallel translations along the x and y directions. Similar calculations were carried out for in-plane rotation. The translation along the x direction is denoted as short slipped translation, while the translation along the y direction is denoted as long slipped translation. If we distort the geometry of the parallel stacked conformer, the symmetry of the system is reduced, which significantly increases the CPU time. In the case of naphthalene and pyrene excimers, we considered B_{2g} , B_{3g} , B_{2u} , and B_{3u} excited states. B_{3g} as well as B_{2g} states are close in energy at the equilibrium distance. In the case of the pyrene excimer, the B_{2g} state is slightly lower in energy than the B_{3g} state. This fact was confirmed by using TD-DFT and RI-CC2 approaches. We performed a similar analysis of potential energy curves for distorted geometries of the naphthalene excimer using the TD-DFT approach. While the geometry of the naphthalene dimer is highly distorted, the RI-CC2 approach diverges in many cases; thus such results are not reported. For the pyrene excimer, the number of basis functions (916) is relatively large. Thus, we report the results for only stacked conformers, in consideration that the optimized structure will not be significantly different from the most stable stacked conformers.

Calculations were carried out by using the Turbomole,³⁹ Molpro,⁴⁰ and ADF⁴¹ suites of programs. All optimized structures were drawn with the Posmol package.⁴² We carried out similar calculations for the benzene dimer employing CIS and CASSCF methods. In both cases, all excited states are repulsive, which clearly demonstrates that dynamic correlation is crucial in our considerations. We decided to use a moderate size basis set, as it is known that a gradual improvement of the basis set substantially improves binding energies of aromatic excimers. The counterpoise corrected binding energies and equilibrium distances are closer to experimental values.⁴³ However, such calculations are feasible for the benzene dimer; for larger aromatic excimers, a gradual improvement of the basis set leads to a significant increase in computing time.

The energy of the charge resonance (CR) state is directly proportional to the difference between the ionization potential (IP) and the electron affinity (EA) of the monomers.⁴⁴ We carried out calculations of IP-EA differences for benzene, naphthalene, anthracene, and pyrene at the TD-DFT (PBE0, PBE, B3LYP, ω PBEh) and RI-CC2 levels of theory.

The PBE0 functional is considered to be a robust functional which performs well for excited state calculations. The issues related to excited states will be discussed later. To check out the role of the self-interaction error in our calculations, we carried out similar calculations using the ω PBEh functional⁴⁵ with the aug-cc-pVDZ basis set. The ω PBEh functional is a long-range corrected PBE functional in which the effect of self-interaction error is significantly reduced. It is noted that the self-interaction error spoils the description of Rydberg states and charge transfers.

RESULTS AND DISCUSSION

The experimental binding energy (BE) for the first singlet excited state of the benzene excimer (B_{1g}) is ~ 0.40 eV.^{46,47} Our calculated BEs tend to be overestimated in comparison with the experimental value.

The best agreement with the experimental BE is obtained at the TD-DFT level combined with the B3LYP functional. The difference does not exceed 0.15 eV. The BE calculated at the CP-corrected RI-CC2/aug-cc-pVQZ level of theory⁴³ is 0.86 eV. The RI-CC2 approach highly overestimates the binding energy. The EOM-CCSD binding energy is slightly lower than the corresponding RI-CC2 value; however, the difference between experimental values is relatively large. Although ground state aromatic systems are properly described by relatively strong π - π interactions, it seems that the RI-CC2 approach overestimates the dispersion energy contribution of the aromatic excimers.^{57–84} In the case of the RI-CC2 method, the benzene excimer is formed for the B_{2u} excited state, which is repulsive at any other level of theory. The CASPT2/aVDZ binding energy is closer to the experimental value; however, the difference is 0.46 eV. It is possible to substantially improve CASPT2/ANO(C,4s3p2d/H,3s2p) results by employing ANO (Atomic Natural Orbital) basis sets.¹³ However, we do not intend to compare different computational methods based on different basis sets. The experimental emission energy for the first excited state of the benzene excimer is 3.94 eV.⁴⁴ Both RI-CC2 and EOM-CCSD methods overestimate the experimental emission energy; however, the relative differences are not as large as in the case of BEs. The emission energies given by the TD-DFT approach are close to the experimental value. The experimental distance between centroids of benzene rings (equilibrium distance) is in the range 3.0–3.5 Å (Table 1).⁸⁵ All equilibrium distances calculated at the TD-DFT level of theory are within this interval. The other approaches underestimate the equilibrium distances; these differences are significant in the case of RI-CC2 and EOM-CCSD methods. It seems that CASPT2 using aug-cc-pVDZ gives quite reliable values of BE, emission energy, and equilibrium distance. It is important to note that the TD-DFT method based on PBE0, PBE, B3LYP, and ω PBEh functionals gives results which are in relatively good agreement with the experimental data. The equilibrium distance and emission energy calculated by Amicangelo¹² are very similar to our results. He carried out TD-DFT calculations employing the B3LYP functional and 6-31+G* basis set (it seems that the similarity between two results is caused by compensation of the errors in Amicangelo's calculations). Krylov and Diri⁸⁶ calculated the equilibrium distance of the benzene excimer using the very accurate EOM-EE-CCSD (equation-of-motion coupled-cluster method for excitation energies) with the 6-31+G(d) basis set. EOM-EE-CCSD provides a properly balanced description of Rydberg and valence states as well as electronic quasi- and exact degeneracies

Table 1. Equilibrium Distances between Centroids, Binding Energies Emission, and Absorption Energies for the Benzene, Naphthalene, Anthracene, and Pyrene Excimers^a

	r_e [Å]	BE [eV](kJ/mol)	emission energy [eV]	absorption energy [eV]
benzene excimer				
TD-DFT (PBE0/aVDZ)	3.05	0.66 (63.4)	4.19	5.46
TD-DFT (PBE/aVDZ)	3.10	0.70 (67.7)	4.23	5.04
TD-DFT (B3LYP/aVDZ)	3.15	0.49 (47.2)	4.15	5.26
RI-CC2/aVDZ	2.85	1.29 (124.7)	4.57	6.27
CASPT2/aVDZ	2.95	0.74 (71.4)	3.71	4.49
EOM-CCSD/aVDZ ^b	2.85	0.91 (87.8)	4.83	6.40
ω PBEh/aVDZ	3.05	0.69 (66.8)	4.15	5.46
exptl. ^c		0.34 (32.8)	3.94	4.79
naphthalene excimer				
TD-DFT (PBE0/aVDZ)	3.25	0.78 (75.6)	3.17	4.42
TD-DFT (PBE/aVDZ)	3.40	0.27 (26.1)	2.79	3.34
TD-DFT (B3LYP/aVDZ)	3.40	0.59 (56.9)	3.25	4.29
RI-CC2/aVDZ	3.00	1.93 (190.3)	2.94	4.70
ω PBEh/aVDZ	3.25	0.77 (73.9)	3.10	4.33
exptl. ^d		0.76 (73.3)	3.13	4.45
anthracene excimer				
TD-DFT (PBE0/aVDZ)	3.40	0.36 (34.7)	3.23	3.91
TD-DFT (PBE/aVDZ)	3.60	0.37 (35.9)	2.93	3.46
TD-DFT (B3LYP/aVDZ)	3.60	0.15 (14.2)	3.31	3.80
RI-CC2/aVDZ	3.05	1.79 (172.4)	2.33	3.78
ω PBEh/aVDZ	3.40	0.60 (57.8)	2.22	3.14
exptl. ^e			2.30	3.27
pyrene excimer				
TD-DFT (PBE0/aVDZ)	3.45	0.71 (68.6)	2.67	3.65
TD-DFT (PBE/aVDZ)	3.60	0.16 (15.9)	2.23	2.57
TD-DFT (B3LYP/aVDZ)	3.60	0.32 (31.0)	3.27	3.49
RI-CC2/aVDZ	3.10	1.93 (186.6)	2.41	4.02
ω PBEh/aVDZ	3.45	0.50 (47.8)	3.14	3.42
exptl. ^f		0.73 (70.4)	2.59	3.70

^aValues are expressed in Å and eV. ^bDiri and Krylov: EOM-EE-CCSD/6-31+G(d) gives $r_e = 3.15$ Å. ^cReferences 44, 47, and 48. ^dReferences 44 and 49. ^eReferences 44 and 50. ^fReferences 44 and 51.

which originate from the electronic transitions between degenerate pairs of molecular orbitals. The equilibrium distance for the benzene excimer at the EOM-EE-CCSD/6-31+G(d) level of theory is 3.15 Å. Even though that the EOM-EE-CCSD is much more accurate than the TD-DFT based on the B3LYP functional, the equilibrium distance for the benzene excimer is identical.

We carried out TD-DFT, RI-CC2, and CASPT2 calculations for distorted geometries of the benzene excimer. These calculations clearly show that the parallel stacked conformer is the most stable form. If we start to distort geometry

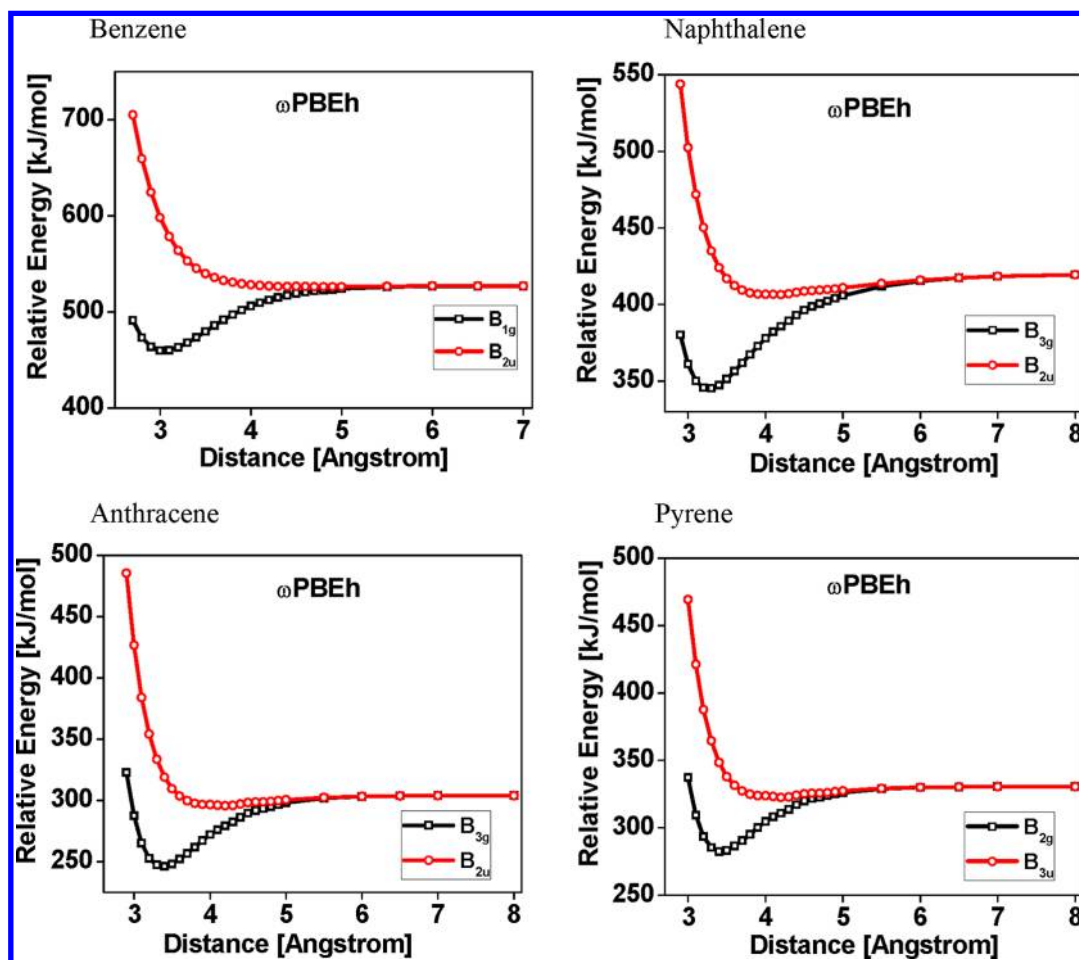


Figure 4. Potential energy curves of the benzene, naphthalene, anthracene, and pyrene excimers calculated at the ω PBEh/aVDZ level of theory. The distance (x axis) denotes the intermolecular distance between monomers (z).

(translation or rotation), the energy of the B_{1g} electronic state always increases. The results of these calculations are presented in the Supporting Information (Figure S1). The long-slipped translation in CASPT2/aVDZ calculations should lead to one electronic excited state. However, the A_g and B_u states have different energies, even if the separation between monomers is large. We calculated all the potential energy curves using active space, which is appropriate for the parallel stacked conformer (Figures S2, S3, S4, and S5). It seems that such active space is invalid for long-slipped translation at the CASPT2/aVDZ level of theory.

We performed similar calculations for singlet excited states of the naphthalene dimer. In this case, we considered B_{3g} , B_{2g} , B_{2u} , and B_{3u} electronic excited states. The naphthalene excimer has not been studied theoretically to such a large extent as the benzene excimer. CASPT2 as well as EOM-CCSD calculations are not practically feasible. We carried out calculations employing the TD-DFT (PBE0, PBE, and B3LYP) and RI-CC2 methods. Similar to the benzene excimer, we performed TD-DFT calculations for distorted geometries of the naphthalene excimer. These computations clearly show that the parallel stacked naphthalene excimer is the most stable conformer. Any deviation from the perfectly stacked geometry leads to an increase in total energy. The emission energy is significantly smaller as compared to the benzene excimer. It is due to a smaller HOMO–LUMO energy gap in the naphthalene dimer in comparison with the benzene dimer.

The RI-CC2 approach overestimates the emission energy for the benzene excimer; however, in the case of the naphthalene excimer the differences between RI-CC2 and TD-DFT are not so large. The BE at the RI-CC2 level of theory is significantly larger (by 1.93 eV) in comparison with the TD-DFT approach. As in the benzene excimer, the RI-CC2 approach overestimates the dispersion energy; thus the naphthalene excimer is likely to be overstabilized. The TD-DFT based on the PBE functional gives a significantly smaller BE in comparison with other DFT functionals. It appears that the TD-DFT approach based on the PBE functional fails when we calculate BE for the naphthalene excimer. The BE of the naphthalene excimer is slightly larger than that of the benzene excimer, however, at the TD-DFT (based on PBE) level, the benzene excimer is significantly more stable. The PBE0 approach is obtained by using the original PBE functional in a hybrid scheme, where the HF ratio is fixed a priori.³⁸ The whole correlation-exchange PBE0 functional can be expressed as

$$E_{XC}^{PBE0} = E_{XC}^{PBE} + \frac{1}{4}(E_X^{HF} - E_X^{PBE})$$

where E_{XC}^{PBE} and E_X^{PBE} are the Generalized Gradient Approximation (GGA) exchange-correlation and exchange contributions, respectively, and E_X^{HF} is the HF exchange. The inclusion of a fraction of the HF exchange energy significantly improves the excitation energies and molecular geometries. On one hand, this is due to the admixture of Hartree–Fock exchange in the

functional, which improves the asymptotic behavior of the exchange-correlation potential by introducing a discontinuity in the potential and by generating proper asymptotic decay. The long-range asymptotic behavior of the PBE functional differs from PBE0 and B3LYP, since the potential energy curves for PBE are very shallow; thus the corresponding BEs are significantly smaller. The equilibrium distance given by the RI-CC2 method is substantially shorter as compared to the TD-DFT approach. It is important to note that the equilibrium distance for the naphthalene excimer is slightly longer than that for the benzene excimer. We calculated the potential energy curves for four different singlet excited states, because in some cases the B_{3g} and B_{2g} states are close in energy. In the case of the RI-CC2 approach, B_{3g} and B_{2g} states are almost degenerate. The TD-DFT method gives a significantly larger separation between these two excited states. It is important to note that during long-slipped translation (along the y direction) another excimer is formed. While we translate a naphthalene ring along the y direction, the symmetry is reduced from D_{2h} to C_{2h} . The excimer formed for the B_{3g} excited state corresponds to the A_u state of C_{2h} symmetry. The excimer related to the B_{2g} excited state corresponds to the A_g state. Those excimers are also identified at the RI-CC2 and TD-DFT (PBE0 and B3LYP) levels of theory. At the TD-DFT (PBE) level, any new excimer cannot be found. The structure of the new excimer is shown in Figure S6.

The equilibrium distances calculated for the anthracene excimer are slightly longer than those of the naphthalene excimer; however, they are very close to equilibrium distances of the pyrene excimer (the difference in r_e does not exceed 0.05 Å). Similarly to the previous cases, the RI-CC2 approach significantly underestimates the r_e distance; the binding energy, 1.79 eV, is much larger than that with the TD-DFT approach. The TD-DFT approach based on the B3LYP functional gives a very small value of the binding energy, 0.15 eV. The potential energy curves for the B_{3g} and B_{2g} states are very shallow at the TD-DFT (B3LYP) level of theory. The binding energies for PBE0 and PBE functionals are substantially larger than that of B3LYP.

For the pyrene excimer, we calculated the potential energy curves for the z translation only (Figure S5). The pyrene dimer is a large molecular system (916 basis functions); thus excited state calculations become computationally very demanding. We computed the potential energy curves for the B_{2g} , B_{3g} , B_{3u} and B_{2u} excited states. Similar to benzene and naphthalene excimers, RI-CC2 significantly overestimates the BE value (1.93 eV) and gives a too short equilibrium distance (3.10 Å) between the monomers. The emission energy is overestimated at the TD-DFT (B3LYP) level of theory. As in the naphthalene excimer case, the BE given by TD-DFT (PBE) is significantly smaller in comparison with other approaches. The equilibrium distances calculated at the TD-DFT level of theory are within the range 3.45–3.60 Å. It is important to note that the B_{2g} excited state is lower in energy than the B_{3g} state, in contrast with the naphthalene excimer.

We carried out calculations for the benzene, naphthalene, anthracene, and pyrene excimers at the ω PBEh/aVDZ level of theory (Figure 4). It is important to note that the ω PBEh/aVDZ results are not significantly different from those of the PBE0/aVDZ. The equilibrium distances for all studied excimers are identical for the ω PBEh and PBE0 functionals. The binding energies are similar for the benzene and naphthalene excimers; the energy difference does not exceed 0.04 eV. However, for

the anthracene and pyrene excimers, the binding energy differences are relatively larger. The largest binding energy difference is 0.24 eV (anthracene excimer). It is due to a better description of long-range correction which substantially reduces the self-interaction error.

The aug-cc-pVDZ basis set gives rise to severe basis set superposition errors. It can be one of the reasons for poor performance of the RI-CC2 approach. Thus, for the benzene excimer, we calculated potential energy curves using the aug-cc-pVTZ basis set. The results of computations are not significantly different from that of aug-cc-pVDZ. The equilibrium distances between monomers are not affected by the basis set improvement. The relative differences between binding energies are not large; the largest difference is 0.08 eV (RI-CC2). The absorption energies are also not significantly different; the largest difference is 0.15 eV (B3LYP). The potential energy curves for aug-cc-pVTZ are presented in the Supporting Information (Figure S7).

Calculations of equilibrium distances for different aromatic excimers allow estimation of the distance between aromatic excimers with an infinite number of benzene rings (such as bilayer infinitely long arenes, bilayer graphene nanoribbons, or bilayer graphene). For this purpose, we estimated the equilibrium distances by using the distance vs $1/n$ plot where the cases $n = 1, 2, 3$, and 4 are benzene, naphthalene, anthracene, and pyrene, respectively (Supporting Information Figure S8). The extrapolated equilibrium distances are within the range of 3.2–3.8 Å. If we discard the highly underestimated RI-CC2 equilibrium distance, the rough estimation of the equilibrium distance between two layers in the first singlet excited state is in the range 3.6–3.8 Å. However, this is a very rough estimation. In this case, we have investigated a very limited number of aromatic excimers, since calculations for much larger aromatic excimers are not feasible to perform. It is possible that when the number of benzene rings is significantly larger, there would be no significant difference in the inter-monomer distances between the case of the ground state and the case of first singlet excitations caused by one exciton. However, such judgment is possible only in the case when results for much larger aromatic excimers are accessible.

The differences between experimental IP and EA for monomers are proportional to the energy of the CR state. The computed IP-EA values are significantly different from the experimental data (Table 2). The TD-DFT approach for the benzene and naphthalene monomers underestimates the IP-EA values; however, the values for the anthracene and pyrene molecules are overestimated. It is important to note that the IP-EA differences are similar for various DFT functionals. It shows that the TD-DFT approach cannot properly describe the

Table 2. IP-EA Values for the Benzene, Naphthalene, Anthracene, and Pyrene Monomers^a

	benzene	naphthalene	anthracene	pyrene
TD-DFT (PBE0)	8.70	7.71	7.68	7.59
TD-DFT (PBE)	8.77	7.66	7.72	7.64
TD-DFT (B3LYP)	8.72	7.65	7.65	7.56
RI-CC2	9.99	10.44	10.76	10.54
ω PBEh	7.47	7.20	7.02	6.95
exptl.	10.32 ^b	7.97 ^b	6.91 ^c	6.93 ^d

^aValues are expressed in eV. ^bReferences 52 and 53. ^cReferences 54 and 55. ^dReferences 54 and 56.

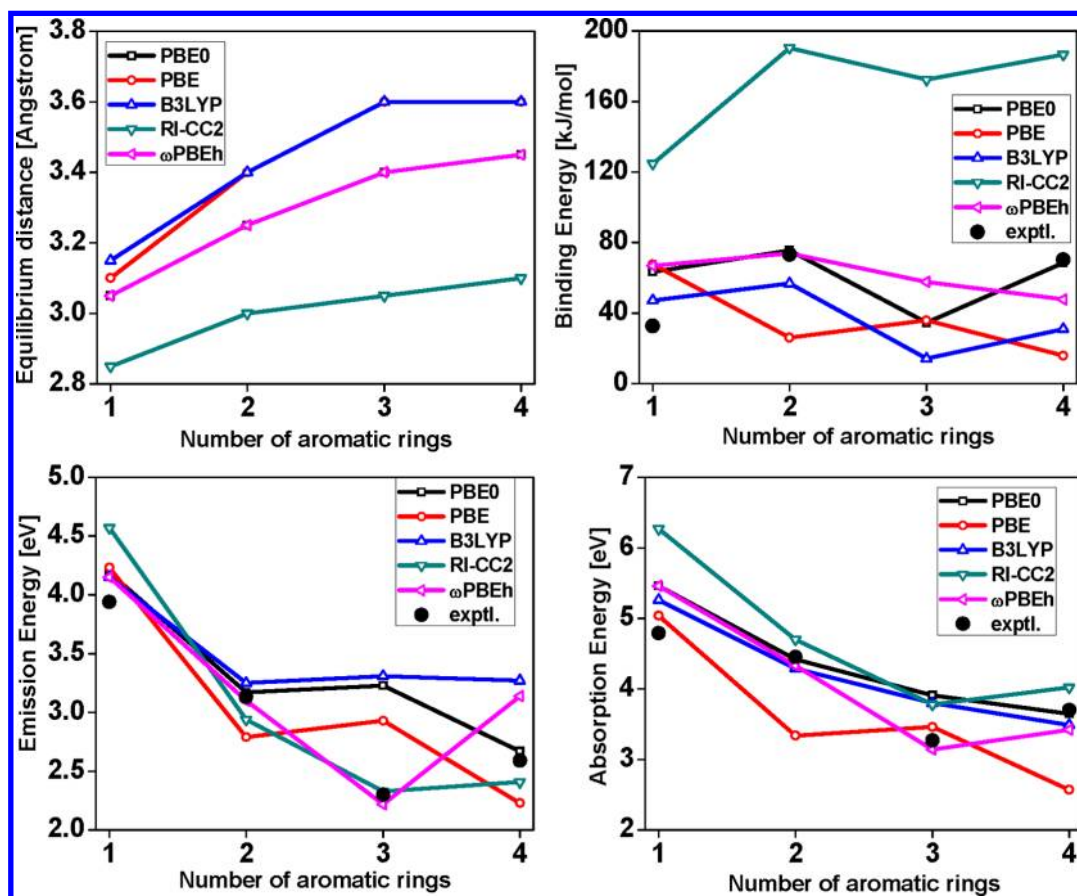


Figure 5. Relations between the number of aromatic rings and equilibrium distances [Å], binding energies [kJ/mol], emission, and absorption energies [eV].

charge resonance (CR) phenomenon. It is known that standard density functionals are not able to describe charge transfer (CT) states properly. The IP-EA values calculated at the RI-CC2 level are highly overestimated (with the exception of the benzene monomer).

Figure 5 presents the relationship of the number of aromatic rings with equilibrium distance, binding energy, emission energy, and absorption energy, respectively. The relation between the number of aromatic rings (n) and equilibrium distances shows that while n increases, the corresponding equilibrium distances converge to a constant value. The equilibrium distances calculated by using the TD-DFT method based on the PBE and B3LYP functionals are similar. The binding energies vary for different numbers of aromatic rings. The RI-CC2 BEs are highly overestimated; however, the trends for RI-CC2 and TD-DFT (PBE0 and B3LYP) are the same. At the TD-DFT (PBE0) and TD-DFT (B3LYP) levels of theory, the absorption energy decreases when the number of aromatic rings increases. The absorption energies given by PBE0 and B3LYP functionals are very close.

The intramolecular charge transfer (CT) states are ubiquitous in weakly interacting molecular systems (e.g., large π electron systems). It is important to note that the TD-DFT calculations should be carried out with great caution for such molecular systems. The TD-DFT calculations based on standard exchange-correlation functionals are not a black-box approach for medium-sized and large systems. In many cases, the PBE0 as well as PBE functionals fail for many similar systems. It is clearly demonstrated in the paper of Goerigk and

Grimme.⁸⁷ They have shown that the PBE0 as well as PBE functionals fail in the proper description of the merocyanine excimer. Very accurate results are obtained using a slightly modified version of the SCS-CIS(D) approach. Fink and co-workers¹⁵ investigated the benzene excimer using different quantum chemical computational approaches. In their case, the TD-DFT approach predicts the charge transfer states at much too low energies. However, such behavior can be observed for the $1E_{1u}$ and $1E_{1g}$ excited states. At the asymptotic limit, the charge transfer state has a very large error of -4.43 eV. For lower singlet excited states of the benzene excimer, the errors are significantly smaller.

The standard procedure of finding the most stable conformers of aromatic excimers is based on the assumption that the monomers are rigid. The potential energy curves for stacked conformations are constructed to determine the equilibrium distance for the selected excited state of the aromatic system. However, we decided to carry out standard geometry optimization of the first singlet excited state (B_{3g}) of the naphthalene and anthracene excimers. Since such calculations are extremely time-consuming, we started from the TD-DFT (PBE0, PBE, B3LYP) geometry optimization with the relatively small DZP basis set. During geometry optimization, the structure of monomers is slightly deformed. The symmetry of the molecular system is decreased from D_{2h} to C_{2v} . To confirm our results, we carried out RI-CC2 and TD-DFT (PBE0, PBE, B3LYP) geometry optimizations with aVDZ basis set. The r distances (described in Figure 6) are slightly

longer as compared with the DZP basis set (Table 3); however, the overall trend is same.

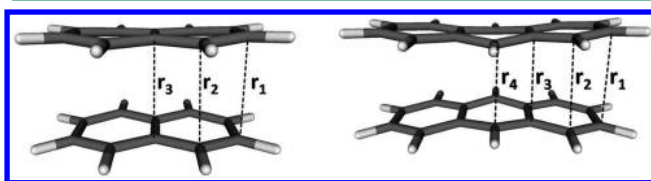


Figure 6. The optimized structures of the naphthalene and anthracene excimers. The r_x ($x = 1, 2, 3, 4$) symbol corresponds to interatomic distances between carbon atoms.

Table 3. The r_1 , r_2 , r_3 , and r_4 Distances [Å] for the Optimized First Singlet Excited State B_{3g} of the Naphthalene and Anthracene Excimers

method	naphthalene excimer			anthracene excimer			
	r_1	r_2	r_3	r_1	r_2	r_3	r_4
PBE0/DZP	3.22	3.09	3.12	3.31	3.29	3.24	3.23
PBE/DZP	3.33	3.22	3.23	3.38	3.34	3.28	3.27
B3LYP/DZP	3.34	3.25	3.27	3.52	3.41	3.34	3.25
PBE0/aVDZ	3.30	3.20	3.22	3.55	3.47	3.36	3.28
PBE/aVDZ	3.42	3.33	3.35	3.59	3.50	3.44	3.38
B3LYP/aVDZ	3.44	3.34	3.36	3.71	3.63	3.58	3.53
RI-CC2/aVDZ	3.06	2.91	2.95	3.33	3.14	3.02	2.79

The deformed monomers have permanent dipole moments, and their orientation is always antiparallel, since the binding energy of the aromatic excimer increases. The B_{3g} excited state is determined by the HOMO→LUMO transition. Figure 7

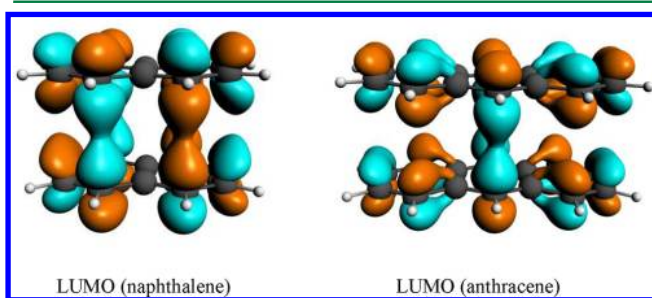


Figure 7. LUMO orbitals of the naphthalene and anthracene dimers.

shows the LUMO orbitals of the naphthalene and anthracene dimers. In the case of the naphthalene dimer, there is a strong overlap between π molecular orbitals which correspond to the shortest r_2 distance. In the case of the anthracene dimer, the largest overlap of the molecular orbitals corresponds to the shortest r_4 distance. The dipole moments [D] of the deformed monomers are reported in Table 4.

DISCUSSION AND CONCLUDING REMARKS

We carried out extensive excited state calculations for the benzene, naphthalene, anthracene, and pyrene dimers. We checked out the reliability of TD-DFT approach for the study of aromatic excimers. For the benzene dimer, we performed a series of accurate post Hartree–Fock methods including EOM-CCSD, CASPT2, and RI-CC2. The RI-CC2 overestimates dispersion forces; thus the corresponding BEs are overestimated and equilibrium distances are significantly under-

Table 4. The Dipole Moments [D] of Naphthalene and Anthracene Monomers^a

system	method	dipole moment [D]
naphthalene	PBE0/DZP	0.14
	PBE/DZP	0.11
	B3LYP/DZP	0.09
	PBE0/aVDZ	0.07
	PBE/aVDZ	0.06
	B3LYP/aVDZ	0.08
	RI-CC2/aVDZ	0.13
anthracene	PBE0/DZP	0.13
	PBE/DZP	0.12
	B3LYP/DZP	0.15
	PBE0/aVDZ	0.10
	PBE/aVDZ	0.08
	B3LYP/aVDZ	0.08
	RI-CC2/aVDZ	0.18

^aThese structures were obtained at the optimized geometry of the first singlet excited state (B_{3g}) of the naphthalene and anthracene excimers.

estimated. The overestimated dispersion energy leads to additional stabilization of the benzene excimer due to much stronger π – π interactions between benzene rings. CASPT2 results are in better agreement with the experimental data; however, the equilibrium distance and emission energy are smaller than the experimental values. It is important to note that the TD-DFT results are not very different from those given by the CASPT2 method, showing that the TD-DFT approach can be a promising tool in the study of larger aromatic excimers. We performed the TD-DFT calculations based on the PBE0, PBE, B3LYP, and ω PBEh functionals. The PBE functional gives relatively good results for the benzene excimer but fails in the case of larger aromatic excimers. The potential energy curves at the TD-DFT level are very shallow; thus the calculated BEs are significantly smaller in comparison with other DFT functionals. The equilibrium distances are close to B3LYP values. The BEs, equilibrium distances, and emission energies calculated at the TD-DFT (PBE0) level are significantly better than the TD-DFT (PBE) results. The TD-DFT (B3LYP) results are in between TD-DFT (PBE0) and TD-DFT (PBE) results. The equilibrium distances are slightly overlenghtened; the emission energy for the pyrene excimer is significantly larger as compared with other approaches. Since the RI-CC2 method overestimates BEs as well as the equilibrium distances, this approach is not suitable for studying aromatic excimers. Aromatic excimers usually have many quasi-degenerate electronic states which give convergence problems in the case of RI-CC2.

It is very important to emphasize the role of the self-interaction error in TD-DFT calculations. The self-interaction error increases with the system size. Thus, calculated results for larger aromatic excimers (anthracene and pyrene) are worse as compared with the benzene and naphthalene excimers. Potential energy curves for the anthracene and pyrene excimers at the PBE/aVDZ level of theory are very shallow. For the GGA functionals (e.g., PBE), the self-interaction error is relatively small but still significant. By their construction, hybrid functionals (e.g., PBE0, B3LYP) incorporate some exact exchange. Hence, the use of a hybrid functional can be viewed as partially correcting for the self-interaction error and the

associated long-range effect. It is evident from our calculations that the performance of hybrid functionals is substantially better than that of GGA. The ω PBEh functional gives slightly better results than PBE0; however, differences are relatively small.

In addition, we carried out geometry optimization of the first singlet excited states (B_{3g}) of the naphthalene and anthracene dimers. The optimized structures are not parallel stacked. During geometry optimization, the structure of monomers is slightly deformed, and the symmetry of the system is decreased from D_{2h} to C_{2v} . We analyzed the r_x ($x = 1, 2, 3, 4$) distances between carbon atoms belonging to different monomers. The shortest interplanar distances correspond to the largest overlap of LUMO orbitals. On the basis of the benzene, naphthalene, anthracene, and pyrene excimers, we might roughly estimate the equilibrium distance for bilayer infinitely long arenes and bilayer graphene nanoribbons in the first singlet excited state, which is roughly estimated to be ~ 3.7 Å according to the extrapolation method; however, since a singlet excitation by one exciton would not significantly change the inter-monomer distance from the ground state, we expect that the first singlet excited systems would still be bound, not separated into two layers.

■ ASSOCIATED CONTENT

● Supporting Information

Figure S1. Potential energy curves for distorted geometries of the benzene and naphthalene excimers. Figure S2. Potential energy curves for the B_{1g} and B_{2u} excited states of the benzene excimer. The distance (x axis) denotes the intermolecular distance between monomers (z). Figure S3. Potential energy curves for the B_{3g} and B_{2u} excited states of the naphthalene excimer. The distance (x axis) denotes the intermolecular distance between monomers (z). Figure S4. Potential energy curves for the B_{3g} and B_{2u} excited states of the anthracene excimer. The distance (x axis) denotes the intermolecular distance between monomers (z). Figure S5. Potential energy curves for the B_{2g} and B_{3u} excited states of the pyrene excimer. The distance (x axis) denotes the intermolecular distance between monomers (z). Figure S6. Second naphthalene excimer formed for short slipped-translation. Figure S7. Potential energy curves for the B_{1g} and B_{2u} states of the benzene excimer. In this case, we employed aug-cc-pVTZ basis set. Figure S8. Extrapolation curves ($1/n$ dependence) for equilibrium distances calculated at the TD-DFT (PBE0, PBE, B3LYP, ω PBEh) and RI-CC2 levels of theory. This material is available free of charge via the Internet at <http://pubs.acs.org>

■ AUTHOR INFORMATION

Corresponding Author

*E-mail: kim@postech.ac.kr.

Present Address

[†]Department of Theoretical Chemistry, Institute of Chemistry, University of Silesia, 9 Szkolna Street, 40-006 Katowice, Poland.

Notes

The authors declare no competing financial interest.

■ ACKNOWLEDGMENTS

This work was supported by NRF (National Honor Scientist Program, WCU: R32-2008-000-10180-0) and KISTI (KSC-2011-G3-02).

■ REFERENCES

- (1) Birks, J. B. *Rep. Prog. Phys.* **1975**, *38*, 903.
- (2) Xu, Z.; Singh, N. J.; Lim, J.; Pan, J.; Kim, H. N.; Park, S.; Kim, K.; Sand, Y. J. *Am. Chem. Soc.* **2009**, *131*, 15528.
- (3) Ahmed, N.; Shirinfar, B.; Youn, I. S.; Bist, A.; Suresh, V.; Kim, K. S. *Chem. Commun.* **2012**, *48*, 2662.
- (4) Somerharju, P. *Chem. Phys. Lipids* **2002**, *116*, 57.
- (5) Wu, C.; Wang, C.; Yan, L.; Yang, C. J. *J. Biomed. Nanotechnol.* **2009**, *5*, 495.
- (6) Conlon, P.; Yang, C. J.; Wu, Y.; Chen, Y.; Martinez, K.; Kim, Y.; Stevens, N.; Marti, A. A.; Jockusch, S.; Turro, N. J.; Tan, W. J. *Am. Chem. Soc.* **2008**, *130*, 336.
- (7) Matsika, S. J. *Phys. Chem. A* **2005**, *109*, 7538.
- (8) Conibear, P. B.; Bagshaw, C. R.; Fajer, P. G.; Kovacs, M.; Malnasi-Csizmadia, A. *Nat. Struct. Biol.* **2003**, *10* (10), 831.
- (9) Förster, T.; Kasper, K. Z. *Phys. Chem.* **1954**, *1*, 275.
- (10) Birks, J. B. *Photophysics of Aromatic Molecules*; Wiley-Interscience: London, 1970; pp 301–371.
- (11) Stevens, B.; Ban, M. I. *Trans. Faraday Soc.* **1964**, *60*, 1515.
- (12) Amicangelo, J. C. J. *Phys. Chem. A* **2005**, *109*, 9174.
- (13) Rocha-Rinza, T.; Vico, L. D.; Vervazov, V.; Roos, B. O. *Chem. Phys. Lett.* **2006**, *426*, 268.
- (14) Huenerbein, R.; Grimme, S. *Chem. Phys.* **2008**, *343*, 362.
- (15) Fink, R. F.; Pfister, J.; Zhao, H. M.; Engels, B. *Chem. Phys.* **2008**, *346*, 275.
- (16) Geim, A. K.; Novoselov, K. S. *Nat. Mater.* **2007**, *6*, 183.
- (17) Castro Neto, A. H.; Guinea, F.; Peres, N. M. R.; Novoselov, K. S.; Geim, A. K. *Rev. Mod. Phys.* **2009**, *81*, 109.
- (18) Kim, K. S.; Zhao, Y.; Jang, H.; Lee, S. Y.; Kim, J. M.; Kim, K. S.; Ahn, J.-H.; Kim, P.; Choi, J.-Y.; Hong, B. H. *Nature* **2009**, *457*, 706.
- (19) Min, S. K.; Kim, W. Y.; Cho, Y.; Kim, K. S. *Nat. Nanotechnol.* **2011**, *6*, 162.
- (20) Bae, S.; Kim, H.; Lee, Y.; Xu, X.; Park, J.-S.; Zheng, Y.; Balakrishnan, J.; Lei, T.; Kim, H. R.; Song, Y. I.; Kim, Y.-J.; Kim, K. S.; Ozyilmaz, B.; Ahn, J.-H.; Hong, B. H.; Iijima, S. *Nat. Nanotechnol.* **2010**, *5*, 574.
- (21) Kim, W. Y.; Kim, K. S. *Nat. Nanotechnol.* **2008**, *3*, 408.
- (22) Elias, D. C.; Nair, R. R.; Mohiuddin, T. M. G.; Morozov, S. V.; Blake, P.; Halsall, M. P.; Ferrari, A. C.; Boukhvalov, D. W.; Katsnelson, M. I.; Geim, A. K.; Novoselov, K. S. *Science* **2009**, *323*, 610.
- (23) Bunch, J. S.; Verbridge, S. S.; Alden, J. S.; van der Zande, A. M.; Parpia, J. M.; Craighead, H. G.; McEuen, P. L. *Nano Lett.* **2008**, *8*, 2458.
- (24) Min, S. K.; Cho, Y.; Mason, D. R.; Lee, J. Y.; Kim, K. S. *J. Phys. Chem. C* **2011**, *115*, 16247.
- (25) Wang, X.; Li, X.; Zhang, L.; Yoon, Y.; Weber, P. K.; Wang, H.; Guo, J.; Dai, H. *Science* **2009**, *324*, 768.
- (26) Park, J.; Lee, W. H.; Huh, S.; Sim, S. H.; Kim, S. B.; Cho, K.; Hong, B. H.; Kim, K. S. *J. Phys. Chem. Lett.* **2011**, *2*, 841.
- (27) Chandra, A. K.; Lim, E. C. *J. Chem. Phys.* **1968**, *48*, 2589.
- (28) Chandra, A. K.; Lim, E. C. *J. Chem. Phys.* **1968**, *49*, 5066.
- (29) Sadygov, R. G.; Lim, E. C. *Chem. Phys. Lett.* **1994**, *225*, 441.
- (30) Celani, P.; Werner, H.-J. *J. Chem. Phys.* **2000**, *112*, 5546.
- (31) Hättig, C.; Weigend, F. *J. Chem. Phys.* **2000**, *113*, 5154.
- (32) Perera, S. A.; Sekino, H.; Bartlett, R. J. *J. Chem. Phys.* **1994**, *101*, 2186.
- (33) Perera, S. A.; Nooijen, M.; Bartlett, R. J. *J. Chem. Phys.* **1996**, *104*, 3290.
- (34) Shirai, S.; Iwata, S.; Tani, T.; Inagaki, S. *J. Phys. Chem. A* **2011**, *115*, 7687.
- (35) Nakano, H. *J. Chem. Phys.* **1993**, *99*, 7983.
- (36) Bauernschmitt, R.; Ahlrichs, R. *Chem. Phys. Lett.* **1996**, *256* (4–5), 454.
- (37) Perdew, J. P.; Burke, K.; Ernzerhof, M. *Phys. Rev. Lett.* **1996**, *77*, 3865.
- (38) Adamo, C.; Barone, V. *J. Chem. Phys.* **1999**, *110*, 6158.
- (39) TURBOMOLE, V6.0; University of Karlsruhe and Forschungszentrum Karlsruhe GmbH: Karlsruhe, Germany, 1989–2007;

TURBOMOLE GmbH: Karlsruhe, Germany, 2007. Available from <http://www.turbomole.com> (accessed November 2012).

- (40) Werner, H.-J.; Knowles, P. J.; Lindh, R.; Manby, F. R.; Schütz, M.; Celani, P.; Korona, T.; Rauhut, G.; Amos, R. D.; Bernhardsson, A.; Berning, A.; Cooper, D. L.; Deegan, M. J. O.; Dobbyn, A. J.; Eckert, F.; Hampel, C.; Hetzer, G.; Lloyd, A. W.; McNicholas, S. J.; Meyer, W.; Mura, M. E.; Nicklass, A.; Palmieri, P.; Pitzer, R.; Schumann, U.; Stoll, H.; Stone, A. J.; Tarroni, R.; Thorsteinsson, T. *MOLPRO*, version 2006.1; Institut für Theoretische Chemie, Universität Stuttgart: Stuttgart, Germany, 2006.
- (41) Baerends, E. J.; Ziegler, T.; Autschbach, J.; Bashford, D.; Bérces, A.; Bickelhaupt, F. M.; Bo, C.; Boerrigter, P. M.; Cavallo, L.; Chong, D. P.; Deng, L.; Dickson, R. M.; Ellis, D. E.; van Faassen, M.; Fan, L.; Fischer, T. H.; Fonseca Guerra, C.; Ghysels, A.; Giammona, A.; van Gisbergen, S. J. A.; Götz, A. W.; Groeneveld, J. A.; Gritsenko, O. V.; Grüning, M.; Gusarov, S.; Harris, F. E.; van den Hoek, P.; Jacob, C. R.; Jacobsen, H.; Jensen, L.; Kaminski, J. W.; van Kessel, G.; Kootstra, F.; Kovalenko, A.; Krykunov, M. V.; van Lenthe, E.; McCormack, D. A.; Michalak, A.; Mitoraj, M.; Neugebauer, J.; Nicu, V. P.; Noodleman, L.; Osinga, V. P.; Patchkovskii, S.; Philipsen, P. H. T.; Post, D.; Pye, C. C.; Ravenek, W.; Rodríguez, J. I.; Ros, P.; Schipper, P. R. T.; Schreckenbach, G.; Seldenthuis, J. S.; Seth, M.; Snijders, J. G.; Solà, M.; Swart, M.; Swerhone, D.; te Velde, G.; Vernooijs, P.; Versluis, L.; Visscher, L.; Visser, O.; Wang, F.; Wesolowski, T. A.; van Wezenbeek, T. S.; Wiesenekker, E. M. G.; Wolff, S. K.; Woo, T. K.; Yakovlev, A. L. *ADF2010*; SCM, Theoretical Chemistry, Vrije Universiteit: Amsterdam, The Netherlands. <http://www.scm.com> (accessed November 2012).
- (42) Lee, S. J.; Chung, H. Y.; Kim, K. S. *Bull. Korean Chem. Soc.* **2004**, *25*, 1061.
- (43) Rocha-Rinza, T.; Christiansen, O. *Chem. Phys. Lett.* **2009**, *482*, 44.
- (44) Azumi, T.; McGlynn, S. P. *J. Chem. Phys.* **1964**, *41*, 3131.
- (45) Henderson, T. M.; Izmaylov, A. F.; Scalmani, G.; Scuseria, G. E. *J. Chem. Phys.* **2009**, *131*, 044108.
- (46) Hirayama, F.; Lipski, S. *J. Chem. Phys.* **1969**, *51*, 1939.
- (47) Cundall, R. B.; Robinson, D. A. *J. Chem. Soc., Faraday Trans. 2* **1972**, *68*, 1133.
- (48) Hiraya, A.; Shobatake, K. *J. Chem. Phys.* **1991**, *94*, 7700.
- (49) George, G. A.; Morris, G. C. *J. Mol. Spectrosc.* **1968**, *26*, 67.
- (50) McVey, J. K.; Shold, D. M.; Yang, N. C. *J. Chem. Phys.* **1976**, *65*, 3375.
- (51) Birks, J.; Dyson, D.; Munro, I. *Proc. R. Soc. London, Ser. A* **1963**, *275*, 575.
- (52) Clark, P. A.; Brogli, F.; Heilbronner, E. *Helv. Chim. Acta* **1972**, *55*, 1415.
- (53) Chen, E. C. M.; Wentworth, W. E. *Mol. Cryst. Liq. Cryst.* **1989**, *1171*, 271.
- (54) Hager, J. W.; Wallace, S. C. *Anal. Chem.* **1988**, *60*, 5.
- (55) Scheidt, J.; Weinkauff, R. *Chem. Phys. Lett.* **1997**, *266*, 201.
- (56) Lyons, L. E.; Morris, G. C.; Warren, L. J. *J. Phys. Chem.* **1968**, *72*, 3677.
- (57) Hunter, C. A.; Sanders, J. K. M. *J. Am. Chem. Soc.* **1990**, *112*, 5525.
- (58) Hunter, C. A. *Chem. Soc. Rev.* **1994**, *23*, 101.
- (59) Hobza, P.; Selzle, H. L.; Schlag, E. W. *J. Am. Chem. Soc.* **1994**, *116*, 3500.
- (60) Pitoňák, M.; Neogady, P.; Rezac, J.; Jurečka, P.; Urban, M.; Hobza, P. *J. Chem. Theory Comput.* **2008**, *4*, 1829.
- (61) Tsuzuki, S.; Honda, K.; Uchimaru, T.; Mikami, M.; Tanabe, K. *J. Am. Chem. Soc.* **2002**, *124*, 104.
- (62) Sinnokrot, M. O.; Sherrill, C. D. *J. Phys. Chem. A* **2004**, *108*, 10200.
- (63) Hohenstein, E. G.; Sherrill, C. D. *J. Phys. Chem. A* **2009**, *113*, 878.
- (64) Grimme, S. *J. Comput. Chem.* **2004**, *25*, 1463.
- (65) Piacenza, M.; Grimme, S. *J. Am. Chem. Soc.* **2005**, *127*, 14841.
- (66) Schwabe, T.; Grimme, S. *Phys. Chem. Chem. Phys.* **2007**, *9*, 3397.
- (67) Janowski, T.; Pulay, P. *Chem. Phys. Lett.* **2007**, *447*, 27.
- (68) Hobza, P.; Selzle, H. L.; Schlag, E. W. *J. Phys. Chem.* **1996**, *100*, 18790.
- (69) Geronimo, I.; Singh, N. J.; Kim, K. S. *J. Chem. Theory Comput.* **2011**, *7*, 825.
- (70) Sinnokrot, O. M.; Sherrill, C. D. *J. Phys. Chem. A* **2006**, *110*, 10656.
- (71) Lee, E. C.; Kim, D.; Jurečka, P.; Tarakeshwar, P.; Hobza, P.; Kim, K. S. *J. Phys. Chem. A* **2007**, *111*, 3446.
- (72) Kim, K. S.; Tarakeshwar, P.; Lee, J. Y. *Chem. Rev.* **2000**, *100*, 4145.
- (73) Kolaski, M.; Kumar, A.; Singh, N. J.; Kim, K. S. *Phys. Chem. Chem. Phys.* **2011**, *13*, 991.
- (74) Das, A.; Jana, A. D.; Seth, S. K.; Dey, B.; Choudhury, S. R.; Kar, T.; Mukhopadhyay, S.; Singh, N. J.; Hwang, I.-C.; Kim, K. S. *J. Phys. Chem. B* **2010**, *114*, 4166.
- (75) Řezáč, J.; Riley, K. E.; Hobza, P. *J. Chem. Theory Comput.* **2011**, *7* (11), 3466.
- (76) Maity, S.; Patwari, G. N.; Sedláč, R.; Hobza, P. *Phys. Chem. Chem. Phys.* **2011**, *13* (37), 16706.
- (77) Riley, K. E.; Pitoňák, M.; Jurečka, P.; Hobza, P. *Chem. Rev.* **2010**, *110* (9), 5023.
- (78) Geng, Y.; Takatani, T.; Hohenstein, E. G.; Sherrill, C. D. *J. Phys. Chem. A* **2010**, *114*, 3576.
- (79) Sherrill, C. D.; Takatani, T.; Hohenstein, E. G. *J. Phys. Chem. A* **2009**, *113*, 10146.
- (80) Ringer, A. L.; Sherrill, C. D. *J. Am. Chem. Soc.* **2009**, *131*, 4574.
- (81) Janowski, T.; Ford, A. R.; Pulay, P. *Mol. Phys.* **2010**, *108*, 249–257.
- (82) Pitoňák, M.; Janowski, T.; Neogady, P.; Pulay, P.; Hobza, P. *J. Chem. Theory Comput.* **2009**, *5*, 1761.
- (83) Huff, E. M.; Pulay, P. *Mol. Phys.* **2009**, *107*, 1197.
- (84) Singh, N. J.; Min, S. K.; Kim, D. Y.; Kim, K. S. *J. Chem. Theory Comput.* **2009**, *5*, 515.
- (85) Förster, T. *Angew. Chem., Int. Ed.* **1969**, *8*, 333.
- (86) Diri, K.; Krylov, A. I. *J. Phys. Chem. A* **2012**, *116*, 653.
- (87) Goerigk, L.; Grimme, S. *ChemPhysChem* **2008**, *9*, 2467.